J. Chem. Eng. Data 1987, 32, 357-362

Vapor–Liquid Equilibrium Measurements for the Ethanol–Acetone System at 372.7, 397.7, and 422.6 K

Scott W. Campbell, Richard A. Wilsak, and George Thodos*
Northwestern University, Evanston, Illinois 60201

Isothermal vapor–liquid equilibrium measurements were experimentally obtained for the ethanol–acetone system at 372.7, 397.7, and 422.6 K. Maximum pressure azeotropic behavior was observed at 397.7 and 422.6 K but not at 372.7 K. The *P–x–y* data resulting from this study were correlated by using the three-suffix Margules equation to represent the excess Gibbs free energy of the liquid phase. Additional data available in the literature at temperatures lower than those examined in the present study were used to establish empirical relationships for the temperature dependence of the excess Gibbs free energy. The four-suffix Margules equation was required to model all of the data for this system. These relationships were used to predict the vapor–liquid equilibrium behavior of the ethanol–acetone system at atmospheric pressure. The results were found to agree well with experimental measurements obtained from the literature.

Experimental measurements for vapor–liquid equilibrium behavior at elevated temperatures and pressures have been, for the most part, restricted to hydrocarbon systems. This situation has resulted from needs that existed in the early development of the petroleum industry. Recent developments in the production of synthetic fuels make it mandatory that, in addition to hydrocarbons, systems containing alcohols, ketones, and aldehydes be investigated since the presence of these polar compounds makes a thermodynamic treatment of these systems more difficult. Before investigating the vapor–liquid equilibrium behavior of multicomponent mixtures containing both polar and nonpolar compounds, it will prove useful to examine a typical constituent binary system comprised of two polar components. In this context, the ethanol–acetone system has been selected for study. For this system isobaric measurements at atmospheric pressure are reported by Amer et al. (*1*), Vinichenko and Susarev (*2*), Hellwig and Van Winkle (*3*), Thayer (*4*), and Duttey as reported by Gmehling and Onken (*5*) and range in temperature between 329.2 and 351.44 K, the normal boiling points of acetone and ethanol, respectively. Isothermal measurements are reported by Shaw and Anderson (*6*) at 313.15 K, Rhim and Park (*7*) for five temperatures ranging from 288.15 to 328.15 K, Vinichenko and Susarev (*2*) at 328.15 K, Gordon and Hines (*8*) at 305.15, 313.15, and 321.15 K, and Chaudhry et al. (*9*) at 323.15 K. From their studies on the ethanol–acetone system, Thomas et al. (*10*) report infinite dilution activity coefficients for acetone in ethanol at 322.5, 335.8, and 348.3 K and for ethanol in acetone at 306.8, 315.2, and 327.7 K. Experimental measurements for the critical temperature locus of this system have been reported by Marshall and Jones (*11*). In order to extend the ranges in temperature and pressure for which experimental information is available, the present study reports isothermal vapor–liquid equilibrium measurements for the ethanol–acetone system at 372.7, 397.7, and 422.6 K.

Experimental Section

The ethanol used in this investigation was supplied by the U.S. Industrial Chemicals Co. and was of reagent grade with a purity of 99.9% by volume. The acetone was supplied by Mallinckrodt and was of spectrophotometric grade with a stated purity of at least 99.5%, the principal impurity being water. The acetone was dehydrated, and both reagents were degassed by using the procedure outlined by Campbell et al. (*12*).

The equipment and procedure used in the present study were outlined by Campbell et al. (*12*). The column of the gas chromatograph was packed with Porapak Q and the resulting chromatograms contained distinct peaks for ethanol and acetone. The experimental uncertainties were estimated to be 0.1 K for temperature, 0.7 kPa for pressure, and 0.005 mole fraction for composition.

Results

Experimental Measurements. The *P–x–y* measurements for the 372.7, 397.7, and 422.6 K isotherms are presented in Table I and shown in Figure 1. These measurements show that no azeotrope exists at 372.7 K; however, maximum-pressure azeotropes were observed at 397.7 and 422.6 K, as shown in this figure. Also included in Table I and Figure 1 are the pure component vapor pressures measured with this experimental facility. The importance of measuring pure component vapor pressures using the same materials and experimental facility used for the vapor–liquid equilibrium measurements has been discussed by Van Ness et al. (*13*).

Treatment of Data. The determination of the activity coefficients using the experimental data was performed in the same manner as reported by Campbell et al. (*12*). The vapor phase was assumed to obey the pressure-explicit virial equation of state truncated after the second term. The values for the second virial coefficients of ethanol and acetone were obtained from the correlation given by Tsonopoulos (*14*). The second virial cross coefficient was calculated by using the method of Tsonopoulos (*14*) with the interaction coefficient k_{ij} taken as 0.05. The saturated liquid volumes of the pure components, V_i^l, were assumed constant in the Poynting correction term and were obtained by using the correlation of Campbell and Thodos (*15*) and the actual density parameters reported by them. The values of the second virial coefficients and the saturated liquid volumes are presented in Table II.

Activity coefficients calculated for each of the experimental measurements are presented in Table I and are shown in Figure 2. These values have been used to obtain the excess Gibbs free energy. To simplify the establishment of the functional dependence of G^E/RT on composition, values of G^E/RT calculated from experimental data were divided by the product of the liquid-phase mole fractions and were plotted against x_1, the mole fraction of ethanol, as shown in Figure 2. The dependence of G^E/RTx_1x_2 upon x_1 is essentially linear and thus may be represented by the three-suffix Margules equation

$$\frac{G^E/RT}{x_1x_2} = \alpha x_2 + \beta x_1 \quad (1)$$

Since $\ln \gamma_i = [\partial(nG^E/RT)/\partial n_i]_{T,P,n_j}$, where n is the total number of moles, the activity coefficients of ethanol and acetone become

$$\ln \gamma_1 = x_2^2[\alpha + 2(\beta - \alpha)x_1] \quad (2)$$

$$\ln \gamma_2 = x_1^2[\beta + 2(\alpha - \beta)x_2] \quad (3)$$

0021-9568/87/1732-0357$01.50/0

Table I. Vapor-Liquid Equilibrium Measurements, Activity Coefficients, and Calculated Pressures and Vapor-Phase Compositions for the Ethanol (1)-Acetone (2) System at 372.7, 397.7, and 422.6 K

	mole fraction				calculated		deviations	
P, kPa	x_1	y_1	ln γ_1	ln γ_2	P, kPa	y_1	ΔP, kPa	y_1
				T = 372.7 K				
366.8	0.000	0.000						
364.0	0.076	0.066	0.350	0.004	364.4	0.068	-0.4	-0.002
361.3	0.129	0.115	0.366	0.003	361.9	0.113	-0.6	0.002
354.7	0.239	0.198	0.270	0.025	354.7	0.197	0.0	0.001
345.1	0.355	0.282	0.198	0.057	344.5	0.281	0.6	0.001
332.7	0.470	0.377	0.169	0.081	331.9	0.364	0.8	0.013
315.8	0.585	0.465	0.109	0.129	316.4	0.452	-0.6	0.013
297.5	0.699	0.564	0.066	0.194	297.7	0.553	-0.2	0.011
277.2	0.796	0.669	0.039	0.247	278.3	0.657	-1.1	0.012
258.6	0.884	0.773	0.012	0.374	257.1	0.777	1.5	-0.004
222.7	1.000	1.000						
				T = 397.7 K				
665.3	0.000	0.000						
666.0	0.021	0.023	0.416	-0.001	666.0	0.022	0.0	0.001
668.1	0.076	0.069	0.227	0.011	666.6	0.076	1.5	-0.007
666.4	0.144	0.130	0.213	0.019	665.6	0.139	0.8	-0.009
661.5	0.233	0.211	0.202	0.026	661.6	0.217	-0.1	-0.006
652.9	0.342	0.305	0.167	0.044	652.9	0.307	0.0	-0.002
640.5	0.453	0.395	0.122	0.078	639.6	0.396	0.9	-0.001
630.2	0.509	0.454	0.127	0.072	631.3	0.441	-1.1	0.013
612.3	0.600	0.536	0.099	0.094	615.1	0.517	-2.8	0.019
589.8	0.718	0.616	0.023	0.226	588.5	0.625	1.3	-0.009
557.4	0.830	0.744	0.013	0.285	555.9	0.746	1.5	-0.002
521.9	0.922	0.877	0.012	0.281	522.1	0.868	-0.2	0.009
487.1	1.000	1.000						
				T = 422.6 K				
1121.4	0.000	0.000						
1127.6	0.047	0.047	0.197	0.004	1126.6	0.050	1.0	-0.003
1131.8	0.109	0.116	0.253	0.000	1131.6	0.113	0.2	0.003
1135.2	0.176	0.177	0.191	0.010	1134.6	0.179	0.6	-0.002
1134.2	0.271	0.264	0.148	0.023	1134.8	0.268	-0.6	-0.004
1130.0	0.376	0.361	0.121	0.039	1129.6	0.362	0.4	-0.001
1119.4	0.476	0.449	0.088	0.063	1119.4	0.450	0.0	-0.001
1102.1	0.587	0.553	0.067	0.087	1101.8	0.548	0.3	0.005
1075.2	0.696	0.659	0.046	0.112	1077.6	0.648	-2.4	0.011
1047.0	0.801	0.758	0.020	0.180	1046.4	0.754	0.6	0.004
1000.8	0.924	0.891	-0.001	0.321	998.0	0.896	2.0	-0.005
960.1	1.000	1.000						

Table II. Second Virial Coefficients, Saturated Liquid Volumes, Constants for the Three-Suffix Margules Equation, and Resulting Root Mean Square Deviations for the Ethanol (1)-Acetone (2) System

								RMS dev	
T, K	B_{11}, cm^3/mol	B_{12}, cm^3/mol	B_{22}, cm^3/mol	V_1^l, cm^3/mol	V_2^l, cm^3/mol	α	β	ΔP, kPa	Δy_1
372.7	-757.6	-656.0	-854.2	64.6	83.8	0.4472	0.4512	0.8	0.008
397.7	-562.3	-519.6	-692.9	67.4	88.3	0.3672	0.4190	1.2	0.009
422.6	-440.0	-425.5	-575.3	70.9	94.0	0.2773	0.3273	1.2	0.005

Although values of α and β could be obtained directly from Figure 2 by a least-squares fit of G^E/RTx_1x_2 to x_1, the approach outlined by Barker (*16*) using only P-x data was adopted. This approach has been examined comprehensively by Abbott and Van Ness (*17*) who found that the use of vapor-phase mole fractions in the data reduction process can lead to distortions in the correlation of the excess Gibbs free energy. Although the basic ideas of Barker's method were retained in the present study, the optimal values of α and β were obtained by using a nonlinear regression routine rather than the numerical approach outlined by Barker. The parameters α and β as well as the resulting root mean square deviations in P and y_1 are given in Table II. Included in Figure 2 are predicted curves for ln γ_1, ln γ_2, and G^E/RTx_1x_2 by use of the values of α and β obtained from the nonlinear regression analysis. Since eq 2 and 3 satisfy the isobaric-isothermal Gibbs-Duhem equation, the predicted curves of Figure 2 are thermodynamically consistent on the assumption that the effect of pressure on the activity coefficients may be neglected. This assumption has been used throughout this study. The thermodynamic consistency of the data is indicated by the conformity of the activity coefficients obtained from the experimental measurements to the calculated curves and their scatter about them. Generally, the data of this study are thermodynamically consistent although some bias appears to exist for the 372.7 K isotherm for ethanol mole fractions between 0.45 and 0.80 and for the 397.7 K isotherm for ethanol mole fractions between 0.05 and 0.25. In Table I, deviations between calculated and experimental values of pressure and vapor-phase mole fraction are presented. Since vapor-phase mole fractions were not used for the establishment of parameters α and β, they present an alternate means for testing the thermodynamic consistency of the data. The deviations in vapor-phase mole fraction, Δy_1, scatter reasonably well around zero with the exception of a portion of the 372.7 K isotherm as shown in Table I.

The error bars shown in Figure 2 were constructed by using estimated uncertainties of 0.005 in composition and 0.7 kPa in pressure. The effect of uncertainty in temperature was not taken into account. These error bars show that any bias in the data is within the estimated uncertainties in the measurements.

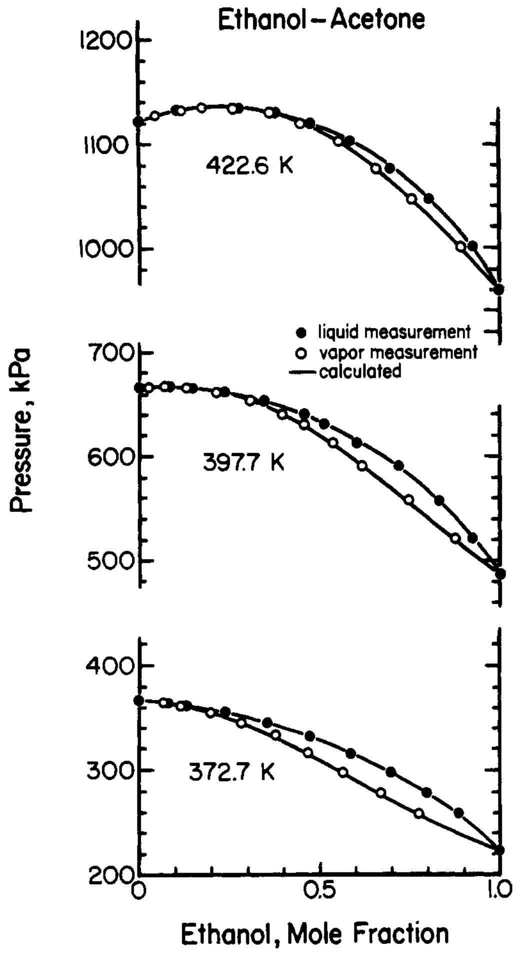

Figure 1. Vapor-liquid equilibrium behavior for the ethanol-acetone system at 372.7, 397.7, and 422.6 K.

Azeotropic Behavior. The atmospheric and subatmospheric measurements reported in the literature do not indicate the existence of azeotropic behavior for temperatures up to 351.44 K, the normal boiling point of ethanol. The data of the present study show that no azeotrope exists at 372.7 K but that maximum-pressure azeotropes exist at 397.7 and 422.6 K. For these two temperatures, the following azeotropic compositions and pressures resulted from a careful examination of the experimental measurements. Also included are the values obtained through the use of the three-suffix Margules equation

	ethanol mole fraction		press., kPa	
T, K	obsd	calcd	obsd	calcd
397.7	0.030	0.073	668.8	667.0
422.6	0.190	0.230	1136.2	1135.3

Comprehensive Treatment of All Available Data

The form of eq 1 assumes a linear dependence of G^E/RTx_1x_2 on composition. This assumption may not always be valid, thus necessitating the introduction of higher order terms. In this context, Chaudhry et al. (*9*) used the five-suffix Margules equation

$$\frac{G^E/RT}{x_1x_2} = \alpha x_2 + \beta x_1 - (\lambda_{21}x_1 + \lambda_{12}x_2)x_1x_2 \tag{4}$$

to correlate their *P*–*x* data for the ethanol–acetone system at 323.15 K. Since the three-suffix Margules equation was applied

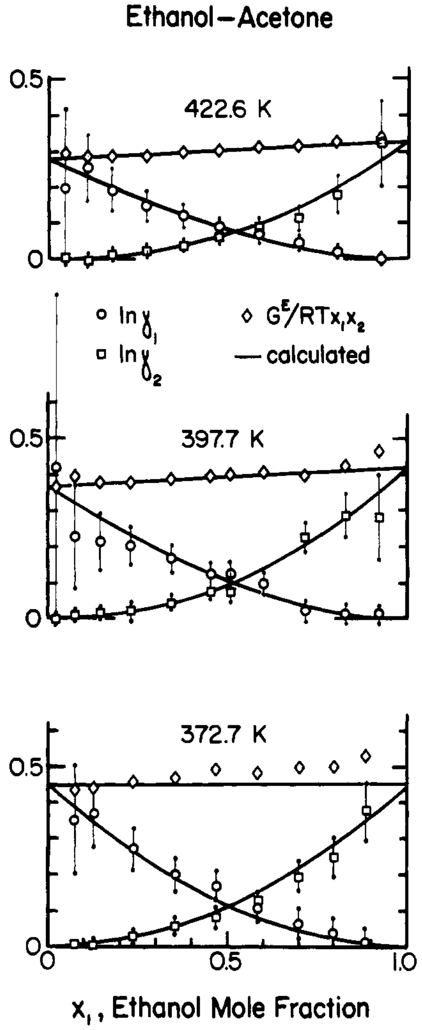

Figure 2. Activity coefficients and excess Gibbs free energies for the ethanol (1)–acetone (2) system at 372.7, 397.7, and 422.6 K.

to the data of the present study and since Chaudhry et al. (*9*) used the five-suffix Margules equation, it is reasonable to investigate the possibility of using the four-suffix Margules equation

$$\frac{G^E/RT}{x_1x_2} = \alpha x_2 + \beta x_1 - \delta x_1x_2 \tag{5}$$

to model the composition dependence of the excess Gibbs free energy. Therefore, the isothermal vapor–liquid equilibrium data of Vinichenko and Susarev (*2*), Gordon and Hines (*8*), Chaudhry et al. (*9*), and those of the present study were fitted to the three-, four-, and five-suffix Margules equations by using Barker's method in order to determine which form is most appropriate for representing all of the data. The data of Rhim and Park (*7*) were not included in this analysis since they did not report pure component vapor pressures. Shaw and Anderson (*6*) did not present their measurements numerically, but instead gave a plot of the activity coefficients vs. composition. Since the values of these activity coefficients could not be reliably read from this plot, their results were not included in the present analysis. The root mean square deviations in pressure and vapor-phase composition for the data included in this analysis are given in Table III. These deviations show that the four-suffix Margules equation is better than the three-suffix Margules equation but that the five-suffix Margules equation is not significantly better than the four-suffix Margules equation. Therefore, eq 5 was selected to represent the excess Gibbs free energy of the ethanol–acetone system for temperatures

Table III. Deviations in Pressure and Vapor-Phase Composition Resulting from the Application of the Three-, Four-, and Five-Suffix Margules Equations to Isothermal Vapor-Liquid Equilibrium Data for the Ethanol-Acetone System and Parameter Values for the Four-Suffix Margules Equation

		3-suffix		4-suffix		5-suffix		eq 5		
T, K	points	ΔP, kPa	Δy_1	ΔP, kPa	Δy_1	ΔP, kPa	Δy_1	α	β	δ
				Gordon and Hines (*8*)						
305.15	14	0.07	0.0098	0.01	0.0096	0.01	0.0096	0.8181	0.8635	0.1315
313.15	14	0.07	0.0063	0.04	0.0056	0.04	0.0058	0.7456	0.7502	0.0800
321.15	14	0.09	0.0052	0.04	0.0046	0.04	0.0046	0.7056	0.7214	0.0988
				Chaudhry et al. (*9*)						
323.15	13	0.100		0.023		0.012		0.7028	0.7770	0.1133
				Vinichenko and Susarev (*2*)						
328.15	8	0.51	0.016	0.37	0.014	0.36	0.014	0.6772	0.7057	0.3441
				This Investigation						
372.7	9	0.8	0.008	0.8	0.008	0.4	0.008	0.4531	0.4610	0.0341
397.7	11	1.2	0.009	1.0	0.009	1.0	0.008	0.3884	0.4456	0.1079
422.6	10	1.2	0.005	1.1	0.004	0.9	0.004	0.2884	0.3421	0.0594

Table IV. Comparison of the Correlation of Van Ness and Abbott and That Given by Eq 5, 7, 8, and 9 with Experimental Vapor-Liquid Equilibrium Data and Excess Enthalpy Data for the Ethanol-Acetone System

Isothermal Vapor-Liquid Equilibrium

		dev in P, %	
investigator	T, K	Van Ness and Abbott	eq 5, 7-9
Gordon and Hines (*8*)	305.15	0.22	0.63
	313.15	1.02	0.40
	321.15	0.77	0.25
Chaudhry et al. (*9*)	323.15	0.20	0.47
Vinichenko and Susarev (*2*)	328.15	1.27	1.00
this investigation	372.7	0.44	0.37
	397.7	1.60	0.33
	422.6	2.29	0.17

Isothermal Excess Enthalpy

		dev in H^E, %	
investigator	T, K	Van Ness and Abbott	eq 5, 7-9
Coomber and Wormald (*20*)	298.15	3.51	3.87
Hirobe (*21*)	298.15	2.27	2.64
Nicolaides and Eckert (*19*)	298.15	0.29	2.31
	323.15	0.18	10.79

between 305.15 and 422.6 K. The optimal values for parameters α, β, and δ in eq 5 are included in Table III.

In order to produce a useful correlation of the available vapor-liquid equilibrium data for the ethanol-acetone system, it is necessary to express the dependence of the excess Gibbs free energy on temperature. Both excess enthalpy data and values of the excess Gibbs free energy derived from vapor-liquid equilibrium data can be used to establish this dependence since they are related through the Gibbs-Helmholtz equation

$$\frac{\partial}{\partial T}\left(\frac{G^E}{RT}\right)_{P,x} = -\frac{H^E}{RT^2} \qquad (6)$$

Van Ness and Abbott (*18*) used the vapor-liquid equilibrium data of Chaudhry et al. (*9*) at 323.15 K and the excess enthalpy data of Nicolaides and Eckert (*19*) at 298.15 and 323.15 K to establish the temperature dependence of the excess Gibbs free energy for the ethanol-acetone system. Using eq 4 and assuming that the excess enthalpy depends linearly on temperature, Van Ness and Abbott obtained temperature dependent relationships for α, β, λ_{12}, and λ_{21}. Their correlation was applied in the present study to the vapor-liquid equilibrium data of the investigators reported in Table III and also to the excess enthalpy data of Coomber and Wormald (*20*), Hirobe (*21*), and Nicolaides and Eckert (*19*). The results of these calculations are given in Table IV and show that the correlation of Van Ness and Abbott (*18*) represents the excess enthalpy data and the vapor-liquid equilibrium data at lower temperatures well but does not represent the vapor-liquid equilibrium data adequately at the higher temperatures. This is not surprising since only data at 323.15 K and lower were used to establish this correlation.

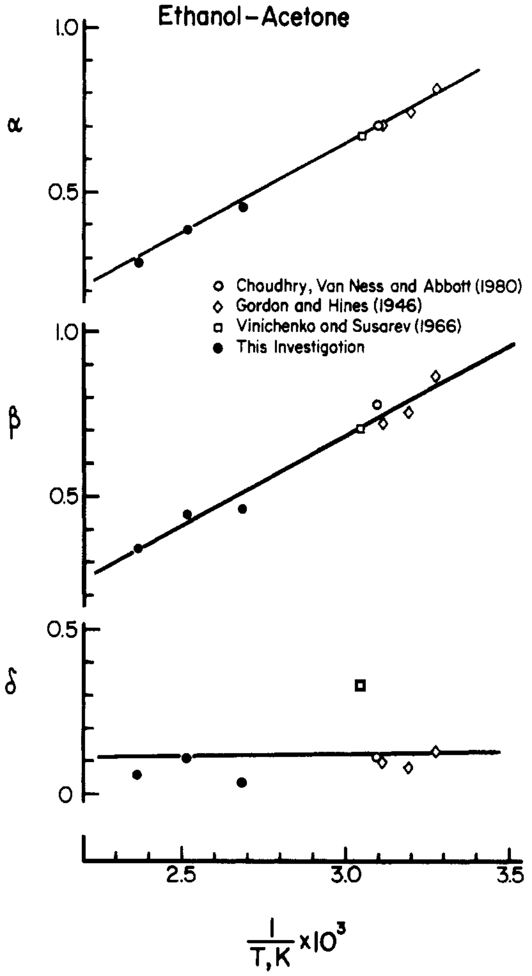

Figure 3. Dependence of parameters α, β, and δ on temperature for the ethanol-acetone system.

In order to represent the vapor-liquid equilibrium data at all temperatures, parameters α, β, and δ given in Table III were plotted vs. reciprocal temperature as shown in Figure 3. From this figure it appears that these parameters relate linearly to reciprocal temperature. Unfortunately, this dependence predicts

Table V. Deviations Resulting from the Use of Eq 5, 7, 8, and 9 in the Calculation of Vapor-Liquid Equilibrium of Ethanol-Acetone at Atmospheric Pressure

investigator	points	root mean square ΔT, K	 Δy_1
Amer et al. (*1*)	9	0.12	
Duttey (*5*)	13	0.12	0.016
Hellwig and Van Winkle (*3*)	9	0.2	0.018
Thayer (*4*)[a]	16	0.45	
Vinichenko and Susarev (*2*)	8	0.29	0.015

[a] Pressure ranged from 98.5 to 99.0 kPa.

that the excess enthalpy is independent of temperature which is inconsistent with the data of Nicolaides and Eckert (*19*) at 298.15 and 323.15 K. An attempt was made to assign a temperature dependence to parameters α, β, and δ such that, when eq 5 was differentiated according to the Gibbs–Helmholtz equation, the parameters in the resulting expression for the excess enthalpy could be completely determined by using excess enthalpy data at only these two temperatures. It was found that no expression of this type adequately fitted the vapor–liquid equilibrium data at the higher temperatures indicating perhaps that the dependence of the excess enthalpy on temperature is more complex than can be derived from data at only two temperatures. Therefore, parameters α, β, and δ were expressed as linear functions of reciprocal temperature as follows:

$$\alpha = \frac{546.3}{T} - 0.9897 \qquad (7)$$

$$\beta = \frac{543.3}{T} - 0.9483 \qquad (8)$$

$$\delta = \frac{15.64}{T} + 0.0759 \qquad (9)$$

The correlation given by eq 5, 7, 8, and 9 was compared to the isothermal vapor–liquid equilibrium data and excess enthalpy data with the results given in Table IV. These results indicate that this correlation fits all of the isothermal vapor–liquid equilibrium data well and even predicts the excess enthalpy data at 298.15 K adequately. However, large deviations result when the correlation is compared to the excess enthalpy measurements at 323.15 K. This is not unexpected since eq 7, 8, and 9 predict that the excess enthalpy is independent of temperature. Therefore, these relationships should only be used for vapor–liquid equilibrium calculations and not for the calculation of heats of mixing.

Prediction of Isobaric Vapor–Liquid Equilibrium Behavior. The correlation for the excess Gibbs free energy has been used to calculate temperature and vapor-phase composition as a function of liquid-phase composition for the ethanol–acetone system at atmospheric pressure. In these calculations it was necessary to express the pure component vapor pressures, saturated liquid volumes, and second virial coefficients as functions of temperature. Pure component vapor pressures were calculated by using the vapor pressure parameters given by Gómez-Nieto and Thodos (*22*) while saturated liquid volumes were obtained by using the actual density parameters given by Campbell and Thodos (*15*). Second virial coefficients were calculated from the correlation of Tsonopoulos (*14*). The results of these vapor–liquid equilibrium calculations are compared to the experimental results of Amer et al. (*1*), Vinichenko and Susarev (*2*), Hellwig and Van Winkle (*3*), and Duttey as reported by Gmehling and Onken (*5*) in Table V and are shown in Figure 4. It is noteworthy that the deviations between the calculated and experimental temperatures and vapor-phase compositions are as low as those reported in the compilation of Gmehling and Onken (*5*).

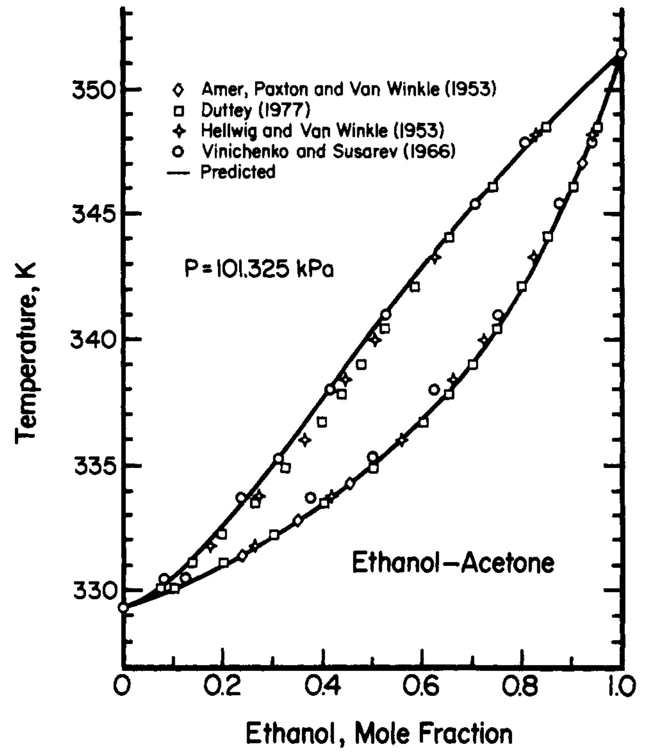

Figure 4. Equilibrium temperature–composition behavior for the ethanol–acetone system at atmospheric pressure.

In addition to these comparisons at a pressure of 101.325 kPa, the correlation was also compared to the data of Thayer (*4*). These data were measured under prevailing atmospheric pressure ranging from 98.5 to 99.0 kPa and thus could not be included in Figure 4. The root mean square deviation between calculated and measured temperatures is included in Table V.

Glossary

B_{ii}	second virial coefficient for component i, cm^3/mol
B_{ij}	second virial cross coefficient, cm^3/mol
G^E	excess Gibbs free energy, J/mol
H^E	excess enthalpy, J/mol
k_{ij}	interaction coefficient for second virial cross coefficient
n	total number of moles
n_i	moles of component i
P	pressure, kPa
R	gas constant, 8314.4 kPa cm^3/(mol K) or 8.3144 J/(mol K)
T	temperature, K
V_i^l	saturated liquid molar volume of pure component i, cm^3/mol
x_i	mole fraction of component i in liquid phase
y_i	mole fraction of component i in vapor phase

Greek Letters

α, β	parameters in three-, four-, and five-suffix Margules equations
γ_i	activity coefficient of component i in the liquid phase
δ	parameter in four-suffix Margules equation
λ_{12}, λ_{21}	parameters in five-suffix Margules equation

Literature Cited

(1) Amer, H. H.; Paxton, R. R.; Van Winkle, M. *Anal. Chem.* **1953**, *25*, 1204.

(2) Vinichenko, I. G.; Susarev, M. P. *J. Appl. Chem. USSR* **1966**, *39*(7), 1475.

(3) Hellwig, L. R.; Van Winkle, M. *Ind. Eng. Chem.* **1953**, *45*, 624.
(4) Thayer, E. F. *J. Phys. Chem.* **1899**, *3*, 36.
(5) Gmehling, J.; Onken, U. *Vapor-Liquid Equilibrium Data Collection*; DECHEMA: Frankfurt/Main, 1977; Vol. I, Part 2a.
(6) Shaw, D. A.; Anderson, T. F. *Ind. Eng. Chem. Fundam.* **1983**, *22*, 79.
(7) Rhim, J. N.; Park, S. S. *Hwahak Konghak* **1975**, *13*(3), 147.
(8) Gordon, A. R.; Hines, W. G. *Can. J. Res.* **1946**, *B24*, 254.
(9) Chaudhry, M. M.; Van Ness, H. C.; Abbott, M. M. *J. Chem. Eng. Data* **1980**, *25*, 254.
(10) Thomas, E. R.; Newman, B. A.; Nicolaides, G. L.; Eckert, C. A. *J. Chem. Eng. Data* **1982**, *27*, 233.
(11) Marshall, W. L.; Jones, E. V. *J. Inorg. Nucl. Chem.* **1974**, *36*, 2319.
(12) Campbell, S. W.; Wilsak, R. A.; Thodos, G. *J. Chem. Eng. Data* **1986**, *31*, 424.
(13) Van Ness, H. C.; Byer, S. M.; Gibbs, R. E. *AIChE J.* **1973**, *19*, 238.
(14) Tsonopoulos, C. *AIChE J.* **1974**, *20*, 263.
(15) Campbell, S. W.; Thodos, G. *Ind. Eng. Chem. Fundam.* **1984**, *23*, 500.
(16) Barker, J. A. *Austral. J. Chem.* **1953**, *6*, 207.
(17) Abbott, M. M.; Van Ness, H. C. *AIChE J.* **1975**, *21*, 62.
(18) Van Ness, H. C.; Abbott, M. M. *Classical Thermodynamics of Non-Electrolyte Solutions*; McGraw-Hill: New York, 1982.
(19) Nicolaides, G. L.; Eckert, C. A. *J. Chem. Eng. Data* **1978**, *23*, 152.
(20) Coomber, B. A.; Wormald, C. J. *J. Chem. Thermodyn.* **1976**, *8*, 793.
(21) Hirobe, H. *J. Fac. Sci., Imp. Univ. Tokyo, Sect. 1* **1926**, *1*, 155.
(22) Gómez-Nieto, M.; Thodos, G. *Can. J. Chem. Eng.* **1977**, *55*, 445.

Received for review August 8, 1986. Accepted May 1, 1987. We extend our gratitude to the Exxon Education Foundation for the financial support of S.W.C.

Calorimetric Study of the Glucose + Ethanol + Water System at High Ethanol Concentrations at 45 °C

Gary L. Bertrand,* Brenda R. Dicknelte, and Oliver C. Sitton

Departments of Chemistry and Chemical Engineering, University of Missouri—Rolla, Rolla, Missouri 65401

Enthalpies of mixing of 50% (w/w) glucose + water solutions with ethanol and aqueous ethanol solutions have been measured at 45 °C. These results have been combined with the enthalpy of dilution in water, partial molar excess enthalpies of water, and the enthalpy of solution of anhydrous glucose in water to obtain the differential enthalpy of solution of glucose in ethanol solutions containing up to 4.5% (w/w) glucose and 15% water. The standard enthalpy of solution in ethanol is considerably more endothermic than in water and is decreased by increasing concentrations of either water or glucose.

As part of a larger study of the thermodynamic properties of sugars in ethanol and ethanol + water mixtures, the differential enthalpy of solution of D-glucose has been determined in ethanol and ethanol-rich aqueous solutions. The rate of solution of anhydrous glucose in these solutions is too slow for accurate calorimetric measurements with the equipment available, so a more complex route to these values was used. A similar technique was used earlier to determine enthalpies of solution of HCl and NaOH in ethanol-rich solutions (*1*). Differential enthalpies of mixing of small amounts of 50% (w/w) aqueous glucose with larger quantities of ethanol, water, and glucose were measured at 45 °C. Final concentrations of glucose were between 0.1 and 4.5%, and final concentrations of water were between 0.1 and 15% (calculated as though the glucose were not present). Combination of these data with partial molar excess enthalpies of water, and the enthalpy of dilution of the glucose solution in water, provides the enthalpy of transfer of glucose from an infinitely dilute state in water to states within the range of compositions given. Further combination with the enthalpy of solution of anhydrous glucose in pure water gives differential enthalpies of solution in the glucose + ethanol + water solutions.

Experimental Section

Materials. D-Glucose was Fisher Certified ACS Dextrose and was used without further purification. Samples for enthalpies of solution were dried for 12 h at 110 °C, but there were no significant differences in measurements on these samples and undried samples. Ethanol was U. S. Industrial Chemicals Punctilious Grade. Singly distilled water in equilibrium with atmospheric carbon dioxide was used for all measurements.

Table I. Enthalpy of Solution of Anhydrous D-Glucose in Water at 45 °C

wt of glucose, g	wt of water, g	ΔH_{soln}, kJ/mol
0.1296	91.24	13.9
0.2027	93.93	13.8
0.3144	91.97	13.5
0.3328	93.10	14.0
0.3582	93.53	13.5
0.3997	92.38	14.0
		av 13.8

Calorimetry. Mixing and dilution measurements were made on a Tronac Model 550 titration calorimeter operating in the isoperibol mode at 45.0 ± 0.1 °C. Titrant solutions of water or 50.0 ± 0.1% glucose were manually injected into weighed solvent mixtures (approximately 95 mL) in increments of 0.1 to 0.5 mL with a 2.5-mL Gilmont micrometer syringe with an accuracy of 0.0002 mL. After delivery of 2.0 mL, the syringe was refilled and the incremental titration continued until a total of 4.0 mL of pure water or 6.0 mL of glucose solution had been injected. At least three heat capacity measurements were performed for each 2-mL series, and calculations of the incremental heats of mixing were based on linear regression of heat capacity vs. volume added. Individual measurements of enthalpy per unit volume are considered to be accurate to 1%. These measurements were converted to a molar basis by using the density of water (0.9902 g/mL) and the measured density (1.206 ± 0.001 g/mL) of the glucose solution.

Enthalpies of solution of anhydrous glucose were measured on a Tronac Model 450 isoperibol titration calorimeter with an ampule adapter. Samples of 0.1–0.4 g were sealed in 1–1.5-mL glass ampules, weighing to within 0.1 mg. Breaking of the ampule into approximately 95 mL of water was bracketed by heat capacity determinations agreeing to within 0.5%. Most of the thermal effect was compensated by using the calibration heater such that the measurements were essentially isothermal. Values were reproducible to within about 1.5%, as has generally been the case for this calorimeter with other sugar samples.

Results and Discussion

The enthalpy of solution of anhydrous D-glucose in water at 45 °C is given in Table I. Any concentration dependence of

0021-9568/87/1732-0362$01.50/0 © 1987 American Chemical Society